12
SLANTWISE CONVECTION

Until now, we have regarded convection as motions arising from an unstable distribution of mass in the vertical direction, with "vertical" meaning along the direction of the gravitational acceleration. On a rotating planet, such as the earth, a more precise definition entails the centrifugal as well as gravitational acceleration, so that "vertical" really means along the direction of *effective* gravity, which is defined to be the sum of the gravitational and centrifugal acceleration vectors.

This raises the important point that physical systems do not respond differently to gravitational and inertial accelerations. Rotating systems experience centrifugal accelerations which the fluid responds to in much the same way as it does to gravity, though the relevant conserved variable is angular momentum instead of temperature or potential temperature. In analogy to purely gravitational convection, there exists a form of convection that arises due to unstable distributions of angular momentum along the vector of the centrifugal acceleration. In the atmosphere, convection may be driven by either or both these mechanisms. In the following sections we develop the theory of purely centrifugal as well as "slantwise" convection and examine observational evidence of slantwise convection in the atmosphere.

12.1 Centrifugal convection

Suppose we have a cylindrical tank of rotating fluid of constant density, as shown in Figure 12.1. We can characterize the motion of the rotating fluid about a central axis by its angular velocity, Ω, or its angular momentum, M:

$$\Omega = \frac{V}{r}, \tag{12.1.1}$$

$$M = rV = r^2\Omega, \tag{12.1.2}$$

where V is the azimuthal velocity and r is the distance from the axis of rotation. Let Ω and M be arbitrary functions of r.

The radial equation of motion in an inviscid flow may be written

$$\frac{du}{dt} = -\alpha_0 \frac{\partial p}{\partial r} + \frac{V^2}{r}, \tag{12.1.3}$$

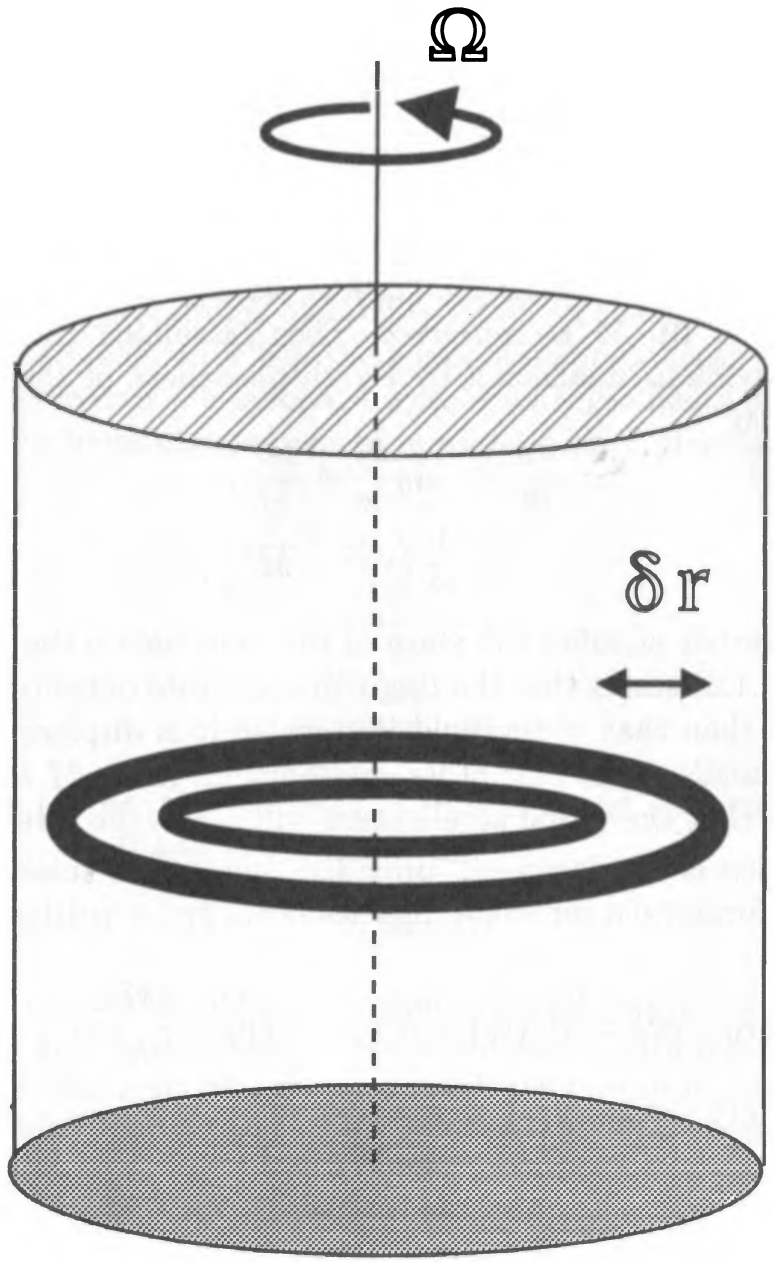

Fig. 12.1 A cylindrical tank of rotating, incompressible fluid showing the distribution of angular momentum and the displacement of an infinitesimal ring of fluid.

where α_0 is the specific volume, here constant. There will be no radial accelerations, and hence the azimuthal flow is *balanced,* so long as

$$\alpha_0 \frac{\partial p}{\partial r} = \frac{V^2}{r} = \frac{M^2}{r^3}. \tag{12.1.4}$$

Now consider a radial displacement of a *ring* of fluid, as shown in Figure 12.1. What will be the acceleration acting on this ring? To calculate this, we shall use the parcel method developed in Chapter 6, except that here we assume that the "parcel" is actually a ring of fluid. As in the classical parcel method, we shall assume that the environment is unperturbed by the displacement of the ring, so that *the pressure field is unaffected by the*

displacement. (This will actually be the case if the cross-sectional area of the ring is infinitesimal.)

The azimuthal component of the equation of motion is

$$\frac{dM}{dt} = -\alpha_0 \frac{\partial p}{\partial \theta}, \tag{12.1.5}$$

where θ is the azimuth. Thus *for inviscid, axially symmetric motions* (for which $\partial p/\partial\theta = 0$), M *is conserved.* Then, assuming that the pressure distribution remains unaffected by the displacement of the ring, (12.1.3) can be written

$$\begin{aligned} \frac{du}{dt} &= -\alpha_0 \frac{\partial \overline{p}}{\partial r} + \frac{M^2}{r^3}, \\ &= \frac{1}{r^3}\left(M^2 - \overline{M}^2\right), \end{aligned} \tag{12.1.6}$$

where the overbar signifies the state of the fluid before the displacement. Equation (12.1.6) states that the ring will accelerate outward if its value of M^2 is larger than that of the fluid into which it is displaced, and inward if its M^2 is smaller than that of its environment. Since M is conserved, it is easily seen that the radial acceleration will act in the direction opposite to the direction of displacement, provided that $\overline{M}^2$ increases with radius. This can be formalized for small displacements δr by writing

$$M^2(r_0 + \delta r) = \overline{M}^2(r_0) = \overline{M}^2(r_0 + \delta r) - \frac{d\overline{M}^2}{dr}\delta r. \tag{12.1.7}$$

Substituting (12.1.7) into (12.1.6) gives

$$\left.\frac{du}{dt}\right|_{r_0+\delta r} = \frac{-1}{r_0^3}\frac{d\overline{M}^2}{dr}\delta r. \tag{12.1.8}$$

Thus if $d\overline{M}^2/dr$ is positive, the acceleration acts in the direction opposite that of the displacement, and the fluid flow is *stable* in this sense. On the other hand, if $d\overline{M}^2/dr$ is negative, the fluid flow is *unstable.* The ensuing motions are said to result from *inertial* or *centrifugal* instability.

Centrifugal instability is nothing more than convective instability, but with inertial accelerations playing the role of gravity. The quantity $(M^2 - \overline{M}^2)/r_0^3$ plays the same role as $g(\theta_{vp} - \theta_{va})/\theta_{va}$, the buoyancy, in gravitational convection. The difference between centrifugal and gravitational convection is the *direction* of acceleration and *the nature of the conserved quantity* from which the acceleration is calculated. In particular, M^2 is conserved for *inviscid, axially symmetric* displacements, whereas θ_v is conserved for all *adiabatic* displacements. By analogy, centrifugal convection is driven by angular momentum fluxes, while gravitational convection is driven by fluxes of heat. The analog to the Rayleigh-Bénard apparatus for

centrifugal convection is a system composed of two concentric cylinders, with the inner cylinder rotating somewhat more rapidly than the outer. Angular momentum fluxes from these cylinders drive centrifugal convection cells that take the form of concentric rings whose vertical spacing is comparable to the radial gap between the cylinders.

Perturbations do not have to be perfectly axially symmetric to experience centrifugal instability. In the atmosphere, one can define more local conditions for centrifugal instability based on the equations of motion phrased on an f plane, on which the horizontal components of the earth's angular velocity vector are ignored together with gradients of the vertical component. The inviscid equations of motion on an f plane are

$$\frac{du}{dt} = -\alpha\frac{\partial p}{\partial x} + fv, \tag{12.1.9}$$

$$\frac{dv}{dt} = -\alpha\frac{\partial p}{\partial y} - fu, \tag{12.1.10}$$

$$\frac{dw}{dt} = -\alpha\frac{\partial p}{\partial z} - g, \tag{12.1.11}$$

where u, v, and w are the eastward, northward, and upward components of velocity, and f is the Coriolis parameter:

$$f \equiv 2\Omega \sin\phi_0, \tag{12.1.12}$$

where Ω is the magnitude of the earth's angular velocity and ϕ_0 is the mean latitude of the area in question. (We are concerned with motions confined to an area over which $\sin\phi$ varies by a small fraction of its mean value.)

Let us further restrict our attention to an atmospheric flow for which there is some direction, call it y', in which the gradient of pressure, multiplied by α, does not vary with height. It is easily verified that the equations of motion, (12.1.9) to (12.1.11) are invariant with respect to a rotation of the coordinate system about the z axis. Thus in the new coordinate frame (x', y', z), (12.1.9) to (12.1.11) may be written

$$\frac{du'}{dt} = -\alpha\frac{\partial p}{\partial x'} + fv', \tag{12.1.13}$$

$$\frac{dv'}{dt} = f(u_g - u'), \tag{12.1.14}$$

$$\frac{dw}{dt} = -\alpha\frac{\partial p}{\partial z} - g, \tag{12.1.15}$$

where u' and v' are the velocities in the x' and y' directions and u_g is a constant:

$$fu_g \equiv -\alpha\frac{\partial p}{\partial y'} = \text{constant}. \tag{12.1.16}$$

The quantity u_g is the *geostrophic wind* in the x' direction and here it is assumed to be constant. Finally, let us have the rotated coordinate

system translate at a constant speed u_g in the x' direction, so that in this new reference frame

$$\begin{aligned} x' &\to x^* + u_g t, \\ y' &\to y^*, \\ z' &\to z^*, \\ u' &\to u^* + u_g, \\ v' &\to v^*, \\ w' &\to w^*. \end{aligned}$$

Then (12.1.13) to (12.1.15) become

$$\frac{du^*}{dt} = -\alpha \frac{\partial p}{\partial x^*} + fv^*, \tag{12.1.17}$$

$$\frac{dv^*}{dt} = -fu^*, \tag{12.1.18}$$

$$\frac{dw^*}{dt} = -\alpha \frac{\partial p}{\partial z^*} - g. \tag{12.1.19}$$

(Hereafter we drop the asterisks and remember that we are in a coordinate system rotated so that the pressure gradient in one direction is constant, and which is translating at speed u_g.)

Since $u = dx/dt$, (12.1.18) can be written

$$\frac{dv}{dt} = -f\frac{dx}{dt},$$

or

$$\frac{dM}{dt} = 0, \tag{12.1.20}$$

where

$$\boxed{M \equiv v + fx.} \tag{12.1.21}$$

The quantity M, the *absolute momentum,* is conserved for inviscid motions on an f plane on which one component of the geostrophic wind is constant. This implies that the only component of the geostrophic wind that varies height is the component in the (new) y direction. But the *thermal wind relation* shows that the temperature gradient is orthogonal to this component of wind. Therefore *the y direction lies along isotherms on a surface of constant pressure, and the x direction lies along the temperature gradient, pointing toward warmer air.*

Suppose we perturb this flow by displacing a two-dimensional "tube" of air in the x direction, as illustrated in Figure 12.2. In order to maintain the condition that M is conserved, it is necessary that the geostrophic wind in the x direction, u_g, remain unperturbed by the displacement. From (12.1.16), this implies that

$$\frac{\partial p'}{\partial y} = 0, \tag{12.1.22}$$

where p' is the pressure perturbation associated with the disturbance. The only disturbances that satisfy (12.1.22) exactly are those for which $\partial/\partial y = 0$, that is, disturbances highly elongated in the y direction (the direction of the mean flow shear). We may write (12.1.17), governing the accelerations in the x direction, as

$$\begin{aligned} \frac{du}{dt} &= -\alpha \frac{\partial p}{\partial x} + fv \\ &= f(v - v_g) \\ &= f(M - M_g), \end{aligned} \tag{12.1.23}$$

where v_g is the geostrophic wind in the x direction, and

$$M_g \equiv v_g + fx, \tag{12.1.24}$$

in analogy with (12.1.21). This quantity is the *geostrophic absolute momentum.* If the displaced tube is elongated in y, then M is conserved, and if, by the parcel hypothesis, the displacement does not perturb the environment, then the distribution of M_g remains fixed. In this case (12.1.23) is exactly analogous to (12.1.6), with the consequence that *the flow is unstable if M_g decreases with x.* This is the special case of centrifugal instability of a straight geostrophic flow on an f plane. In gravitational convection, conservation of some adiabatic invariant (such as θ_v) means that the vertical pressure gradient and gravity will not generally be in balance when a parcel is displaced vertically; if the resulting acceleration is in the same direction as the displacement, the flow is said to be unstable to (gravitational) convection. In parcel theory, we calculate the vertical pressure gradient by assuming that the mass of the displaced parcel is so small that the pressure distribution is unaffected by the displacement.

Likewise, in the case of centrifugal convection, conservation of some angular momentumlike invariant means that when a ring of fluid is displaced in a direction orthogonal to the axis of rotation, the pressure gradient and the centrifugal (or Coriolis) acceleration will not generally be in balance, and if the net acceleration is in the same direction as the displacement, the flow is said to be unstable to centrifugal convection. In parcel theory, we again calculate the pressure gradient by assuming that it is unaffected by the convection.

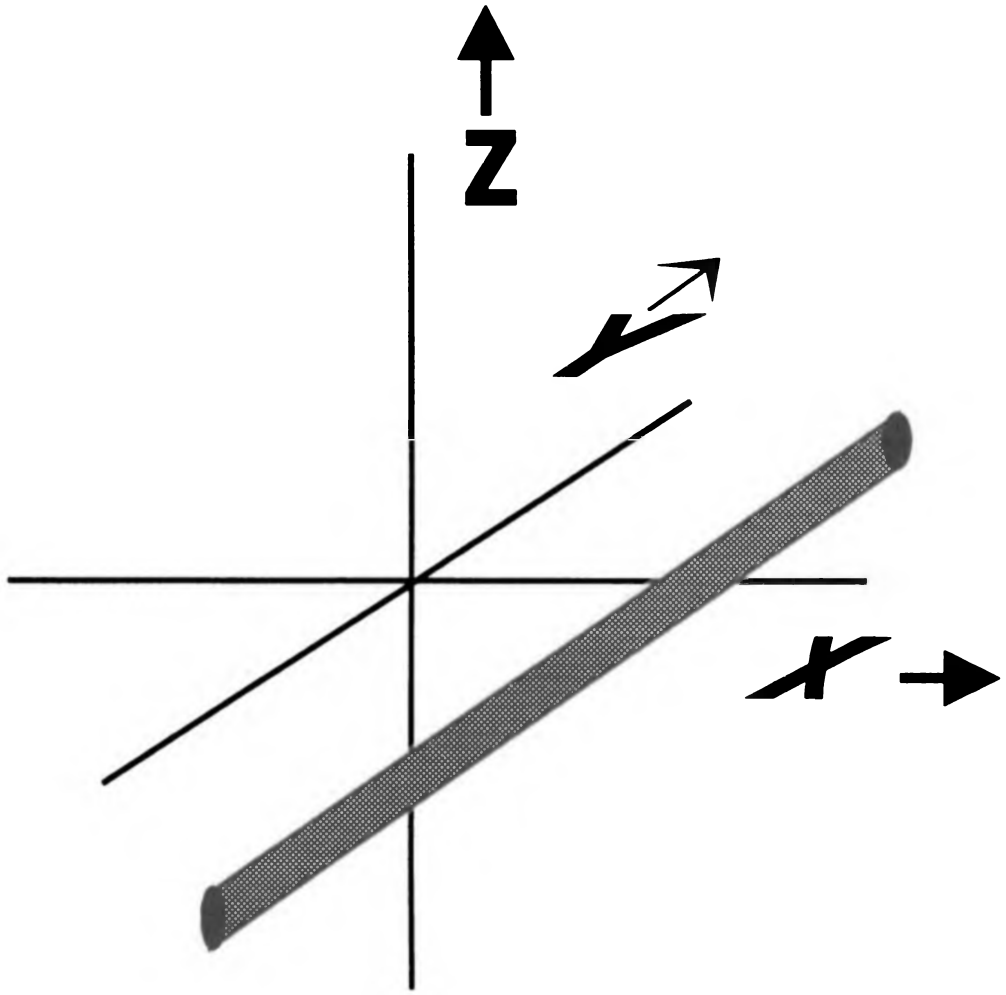

Fig. 12.2 A quasi-two-dimensional "tube" of air, with the y coordinate defined to run along its axis.

12.2 Theory of slantwise convection[1]

Suppose we take the "tube" of air in the last example and displace it vertically as well as horizontally, once again neglecting pressure perturbations arising from the displacement. Then the equation governing horizontal accelerations of the parcel is (12.1.23), while the vertical acceleration is governed by

$$\frac{dw}{dt} = \frac{g(\alpha_t - \alpha_e)}{\alpha_e}, \tag{12.2.1}$$

where α_t is the specific volume of the tube and α_e is that of its environment. We would like to rephrase (12.2.1) in terms of *conserved variables,* to make it look more like (12.1.23). This we can do using Maxwell's relations, developed in Section 4.5. Assuming that $\alpha_t - \alpha_e$ is small compared to α_e, and recognizing that the difference $\alpha_t - \alpha_e$ is to be taken at constant pressure, and regarding α as a function of pressure, entropy, and water content,

[1] The development in this section closely follows that of Emanuel (1983a,b).

then

$$(\alpha_t - \alpha_e)_p \simeq \left(\frac{\partial \alpha}{\partial s}\right)_{p,r_T} (s_t - s_e) + \left(\frac{\partial \alpha}{\partial r_T}\right)_{p,s} (r_{Tt} - r_{Te}), \tag{12.2.2}$$

where s and r_T are the entropy and total water content. The quantity s should be interpreted as the dry entropy if the air is unsaturated and the moist entropy if otherwise. To streamline the following development, we hereafter neglect the contribution of r_T to specific volume, though this is not necessary. Thus, we will neglect the last term in (12.2.2) and replace the specific volume, α, by the specific volume of dry air, α_d. Then (12.2.2) becomes

$$(\alpha_t - \alpha_e)_p \simeq \left(\frac{\partial \alpha_d}{\partial s}\right)_p (s_t - s_e). \tag{12.2.3}$$

Using one of Maxwell's relations, (4.5.30), this can be written

$$(\alpha_t - \alpha_e)_p \simeq \left(\frac{\partial T}{\partial p}\right)_s (s_t - s_e). \tag{12.2.4}$$

Using this and the hydrostatic approximation, (12.2.1) becomes

$$\frac{dw}{dt} \simeq \Gamma(s_t - s_e), \tag{12.2.5}$$

where

$$\Gamma \equiv \begin{cases} -\left(\frac{\partial T}{\partial z}\right)_{s_d} = \frac{g}{c_p} = & \text{dry adiabatic lapse rate,} \\ & \quad \text{unsaturated tube,} \\ -\left(\frac{\partial T}{\partial z}\right)_{s^*} = & \text{moist adiabatic lapse rate,} \\ & \quad \text{saturated tube,} \end{cases} \tag{12.2.6}$$

$$s = \begin{cases} c_p \ln \theta & \text{unsaturated tube,} \\ c_p \ln \theta_e^* & \text{saturated tube,} \end{cases} \tag{12.2.7}$$

where θ_e^* is the value of the equivalent potential temperature air would have if it were saturated at the same pressure and temperature. Since θ is conserved in dry adiabatic displacements and θ_e^* is conserved in moist adiabatic displacements, s_t is always conserved following the displacement of the tube, provided that the displacement is reversible.

In summary, the parcel equations for the tube aligned in the direction of the mean-state isotherms on isobaric surfaces are:

$$\frac{du}{dt} = f(M_t - M_g) \tag{12.2.8}$$

and

$$\frac{dw}{dt} = \Gamma(s_t - s_e), \tag{12.2.9}$$

with Γ and s given by (12.2.6) and (12.2.7).

One can immediately see the analogy between these two equations. In both cases, the accelerations are proportional to the difference between a quantity conserved in the displacement of the tube and the same quantity in the tube's environment. (But remember that M is only conserved for a "tube" of air elongated in the direction of the thermal wind.) This is a manifestation of the dynamic equivalence of inertial and gravitational accelerations.

Now consider a fairly typical atmospheric condition in which the temperature increases in the x direction in the troposphere (Northern Hemisphere). Associated with this is a flow in the y direction in thermal wind balance, so that v_g (and therefore M_g) increases with altitude in the troposphere. (There may also be an x component u_g, but under the conditions imposed here this must be constant. We consider ourselves to be in a coordinate system moving in the x direction at velocity u_g.)

We will impose two conditions on the stability of the flow: that it be stable to *both* gravitational and centrifugal instabilities. From (12.2.8) this means that M_g must increase in the x direction:

$$\frac{\partial M_g}{\partial x} = f + \frac{\partial v_g}{\partial x} > 0. \tag{12.2.10}$$

This is simply a statement that the geostrophic absolute vorticity must have the same sign as f (e.g., positive in the Northern Hemisphere). The requirement of gravitational stability, from (12.2.9), is that the relevant form of entropy increase upward.

It can now be demonstrated that this flow nevertheless may be unstable to *slantwise convection.*

First consider the distributions of M and s shown in Figure 12.3. As in the case of conditional gravitational instability, *we shall examine the stability of the atmosphere to finite displacements of a particular sample (in this case, "tube") of air.*

We note that an upward displacement of the tube, by the conditions imposed in the example, leads to a downward acceleration, since $s_t - s_e$ is a negative quantity above the position of the tube. Similarly, horizontal displacements lead to accelerations back toward the initial position.

But because of the baroclinity of the atmosphere, the quantity s_e increases in the x direction and the quantity M_g increases vertically. Thus, in this example, *M_g and s_e both increase upward and in the positive x direction.* Surfaces of constant M_g and s_e therefore slope upward in the negative x direction.

Consider the environmental M_g and s_e surfaces that happen to pass through the sample, as shown in Figure 12.3. This particular M_g surface is one along which the displaced tube experiences no horizontal acceleration, since its M value, which is conserved in the displacement, will always be the same as its environment. Similarly, the particular s surface is one along

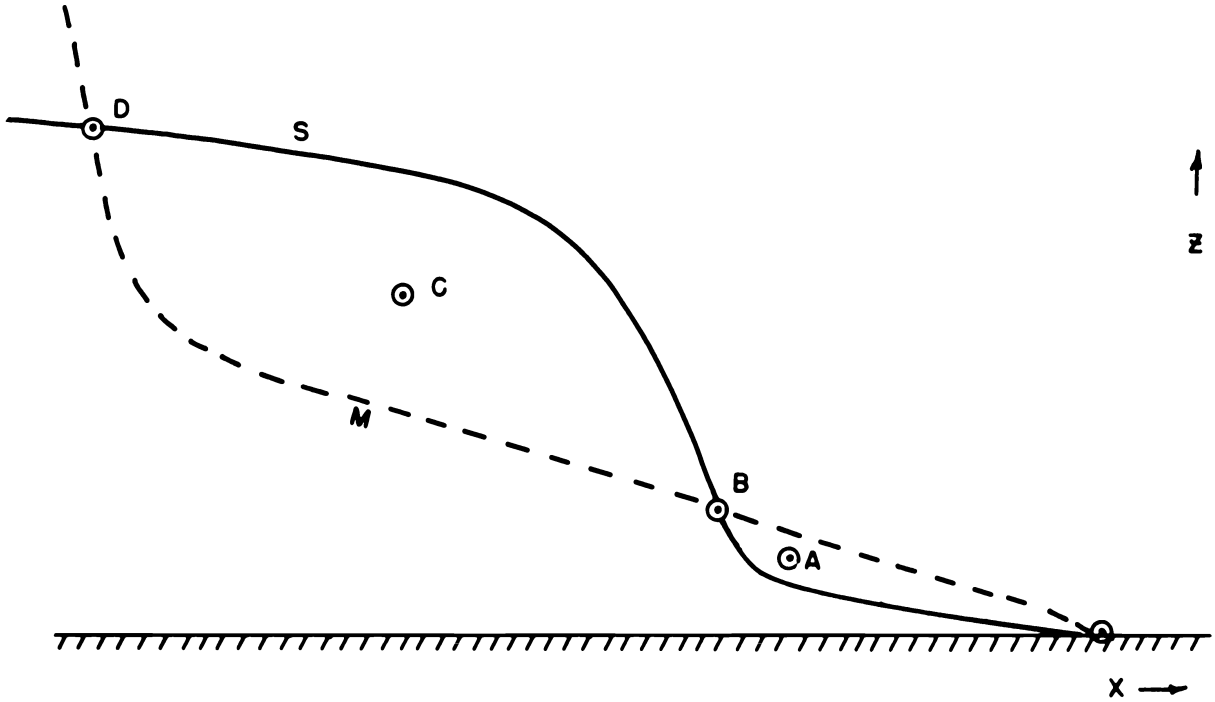

Fig. 12.3 Hypothetical distributions of M (dashed line) and neutral-buoyancy (solid line) surfaces for a tube located at the lower right. Domain is approximately 100 × 10 km.

which the displaced tube experiences no vertical acceleration. (This is, in fact, a more general definition of the s surface associated with the sample: It is one along which the reversibly displaced tube feels no buoyancy force.)

It is evident that *the tube, when displaced an arbitrary distance in some arbitrary direction, will accelerate vertically toward its s surface and horizontally toward its M surface.*

By this simple rule, if our sample tube is displaced to position A in Figure 12.3, it will experience a downward and rightward acceleration which acts to return it to its initial position. If it is displaced to B, however, it experiences no acceleration. When displaced beyond B to, say, C, it is subjected to an upward and leftward acceleration *away* from its initial position. Finally, at D, the tube experiences no acceleration. It is seen that the initial point and point D are stable equilibria, while point B is an unstable equilibrium.

The state of the atmosphere represented in Figure 12.3 is said to be one of *conditional instability to slantwise convection.* The instability is conditional on the sample tube being displaced beyond point B, which may be called the *point of free convection.* This state is in every way analogous to the state of conditional instability to purely gravitational convection, but we must move from one to two dimensions in considering the stability of the atmosphere, and we must consider a one-dimensional "tube" rather than a zero-dimensional "point" of air.

What is the magnitude and geometry of slantwise convection? Clearly, from Figure 12.3, the ascending air will travel somewhere between its

"home" M and s surfaces, but where, precisely? Here it is instructive to consider a very simple example of an atmosphere that is unstable to dry slantwise convection, with the geometry of M and s surfaces shown in Figure 12.4. Let M and s vary in a simple way given by

$$M = \overline{v}_z z + \overline{\eta} x, \tag{12.2.11}$$

$$s = s_0 + \frac{c_p}{g} N^2 z + \overline{s}_x x, \tag{12.2.12}$$

where $\overline{v}_z$, $\overline{\eta}$, $\overline{s}_x$, s_0, and N^2 are all constant. If this basic state is stationary, then the thermal wind equation must be obeyed. This takes the form

$$f\frac{\partial M}{\partial z} = \Gamma\frac{\partial s}{\partial x} = \frac{g}{c_p}\frac{\partial s}{\partial x}. \tag{12.2.13}$$

Comparing (12.2.13) with (12.2.11) and (12.2.12) shows that

$$\overline{s}_x = \frac{c_p}{g} f \overline{v}_z. \tag{12.2.14}$$

Substituting the distributions (12.2.11) and (12.2.12) into the tube equations (12.2.8) and (12.2.9) and using (12.2.14) gives, for a sample tube initially located at $x = z = 0$,

$$\frac{du}{dt} = \frac{d^2x}{dt^2} = -f\left(\overline{v}_z z + \overline{\eta} x\right), \tag{12.2.15}$$

$$\frac{dw}{dt} = \frac{d^2z}{dt^2} = -N^2 z - f\overline{v}_z x. \tag{12.2.16}$$

Eliminating the variable z from (12.2.15) and (12.2.16) gives

$$\frac{d^4x}{dt^4} + \left(N^2 + f\overline{\eta}\right)\frac{d^2x}{dt^2} + \left(f\overline{\eta}N^2 - f^2\overline{v}_z^2\right)x = 0 \qquad (z < H). \tag{12.2.17}$$

This is valid up until the point where $z = H$, at which $dz/dt = 0$ and thus, from (12.2.15),

$$\frac{d^2x}{dt^2} = -f\left(\overline{v}_z H + \overline{\eta} x\right) \qquad (z = H). \tag{12.2.18}$$

The solution of (12.2.17) that satisfies $u = w = 0$ at $x = x_0$, $z = z_0$ is

$$x = -c_1 \cosh \sigma_1 t + c_2 \cos \sigma_2 t, \tag{12.2.19}$$

$$z = c_3 \cosh \sigma_1 t + c_4 \cos \sigma_2 t, \tag{12.2.20}$$

where σ_1 and σ_2 are the positive real roots of

$$\sigma_1^2 = \frac{1}{2}\left[\sqrt{\left(N^2 - f\overline{\eta}\right)^2 + 4f^2\overline{v}_z^2} - \left(N^2 + f\overline{\eta}\right)\right], \tag{12.2.21}$$

$$\sigma_2^2 = \frac{1}{2}\left[\sqrt{\left(N^2 - f\overline{\eta}\right)^2 + 4f^2\overline{v}_z^2} + N^2 + f\overline{\eta}\right], \tag{12.2.22}$$

and c_n are constants defined

$$\begin{aligned} c_1 &\equiv \left[f\overline{v}_z z_0 + (f\overline{\eta} - \sigma_2^2)x_0\right]/(\sigma_1^2 + \sigma_2^2), \\ c_2 &\equiv \left[f\overline{v}_z z_0 + (f\overline{\eta} + \sigma_1^2)x_0\right]/(\sigma_1^2 + \sigma_2^2), \\ c_3 &\equiv (f\overline{\eta} + \sigma_1^2)c_1/f\overline{v}_z, \\ c_4 &\equiv -(f\overline{\eta} - \sigma_2^2)c_2/f\overline{v}_z. \end{aligned} \tag{12.2.23}$$

Thus, from (12.2.19) and (12.2.20), the sample tube executes a complex trajectory, accelerating in the negative x and positive z directions and also oscillating about this trajectory. The oscillatory part will, however, vanish if we choose the slope of the initial displacement just right so that c_2 (and thus c_4) vanish; that is, from (12.2.23) and (12.2.21),

$$\begin{aligned} z_0 &= -x_0\left[\sqrt{(N^2 - f\overline{\eta})^2 + 4f^2\overline{v}_z^2} - (N^2 - f\overline{\eta})\right]/2f\overline{v}_z \\ &\equiv -\beta x_0. \end{aligned} \tag{12.2.24}$$

In this case, $c_2 = c_4 = 0$, $c_1 = x_0$, and $c_3 = z_0$. Then differentiating (12.2.19) and (12.2.20) in time also yields

$$u = x_0\sigma_1 \sinh \sigma_1 t = -\sigma_1\sqrt{x^2 - x_0^2}, \tag{12.2.25}$$

$$w = z_0\sigma_1 \sinh \sigma_1 t = \frac{z_0}{x_0}u, \tag{12.2.26}$$

where z_0/x_0 is given by (12.2.24). Thus, in the limit of vanishing initial displacement,

$$\begin{aligned} u &= -\sigma_1 x, \\ w &= \beta\sigma_1 x, \end{aligned}$$

or, equivalently,

$$u = -\frac{\sigma_1 z}{\beta}, \tag{12.2.27}$$

$$w = \sigma_1 z. \tag{12.2.28}$$

Thus the tube accelerates upward and leftward along a trajectory whose slope is

$$\begin{aligned} \beta &\equiv \frac{z_0}{x_0} \\ &= \frac{\left[\sqrt{(N^2 - f\overline{\eta})^2 + 4f^2\overline{v}_z^2} - (N^2 - f\overline{\eta})\right]}{2f\overline{v}_z}. \end{aligned} \tag{12.2.29}$$

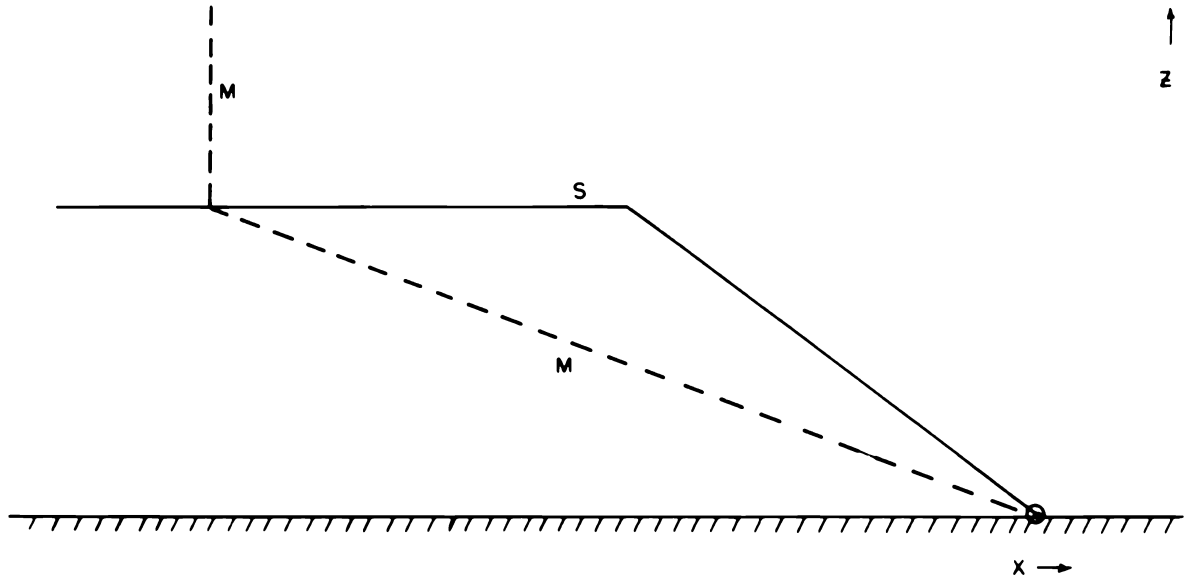

Fig. 12.4 Configuration of M (dashed line) and s (solid line) surfaces used in the calculation of a sample tube's motion, as described in text.

Now all of this clearly pertains only to the case that σ_1, given by (12.2.21), is real. The condition for this to be so is

$$f^2\overline{v}_z^2 > f\overline{\eta}N^2,$$

or

$$\boxed{Ri < \frac{f}{\overline{\eta}},} \tag{12.2.30}$$

where

$$Ri \equiv \frac{N^2}{\overline{v}_z^2}. \tag{12.2.31}$$

The dimensionless quantity Ri is the Richardson number. Thus the criteria for slantwise convection in an unsaturated atmosphere with straight geostrophic flow is just that the Richardson number be smaller than f divided by the absolute vorticity. Instability is favored by low static stability, strong vertical shear, and anticyclonic relative vorticity.

A large simplification of this solution occurs if

$$\frac{f\overline{v}_z}{N^2} \ll 1. \tag{12.2.32}$$

In that case, from (12.2.21) and (12.2.29),

$$\sigma_1^2 \simeq \frac{f^2\overline{v}_z^2}{N^2} - f\overline{\eta} = f^2\left(\frac{1}{Ri} - \frac{\overline{\eta}}{f}\right) \tag{12.2.33}$$

and

$$\beta = -\frac{z_0}{x_0} = \frac{f\overline{v}_z}{N^2} = \frac{f}{N}\frac{1}{\sqrt{Ri}}. \tag{12.2.34}$$

Comparison of (12.2.34) with (12.2.12) and (12.2.14) shows that in this case, the slope of the motion is identical with that of surfaces of constant s (isentropes, in this example). Also, (12.2.16) gives

$$\frac{dw}{dt} = \frac{d^2z}{dt^2} \simeq 0$$

in this limit, so the motion is hydrostatic. We may generalize from this finding, and state that *when the slope of the s surface associated with a particular tube is small, the motion is hydrostatic and slantwise convection occurs very nearly along the s surface.*

When the ascending tube reaches $z = H$, its horizontal and vertical velocities will be, by (12.2.27) and (12.2.28),

$$u = -\frac{\sigma_1 H}{\beta}, \tag{12.2.35}$$

$$w = \sigma_1 H. \tag{12.2.36}$$

Thereafter, w will be zero because of the upper boundary, but the tube will continue to accelerate in the negative x direction, at a rate given by (12.2.18). The solution to this equation with the initial condition $w = 0$, $u = -\sigma_1 H/\beta$ is the negative root of

$$u^2 = -f\overline{\eta}x^2 - 2fv_0 x - \frac{Hfv_0}{\beta}, \tag{12.2.37}$$

where $v_0 \equiv \overline{v}_z H$ is the value of v at $z = H$. The maximum value of u^2 is

$$u^2_{\max} = \frac{fv_0^2}{\overline{\eta}} - \frac{Hfv_0}{\beta},$$

occurring at (12.2.38)

$$\boxed{x_{\max} = -\frac{v_0}{\overline{\eta}}.}$$

This is just the point at which the M surface intersects the tropopause, $z = H$. In the hydrostatic limit, $\beta = f\overline{v}_z/N^2$ and thus

$$\boxed{u^2_{\max} = v_0^2\left(\frac{f}{\overline{\eta}} - Ri\right).} \tag{12.2.39}$$

Unless the instability is marginal, then, the horizontal velocities associated with the instability will be comparable to those of the mean flow.

If the atmosphere is completely saturated, then this analysis also works, but with N replaced by the moist buoyancy frequency, N_m, defined by Eq. (6.2.10).

This analysis shows that slantwise convection takes the form of thin sheets or tubes of air accelerating along trajectories in between the M and s surfaces, but much closer to the latter if the s surfaces have a small slope, in which case the hydrostatic approximation works well. Unless the instability is marginal, slantwise convection may attain velocities comparable to those of the baroclinic flow in which it occurs.

In nature, we might expect such a flow to become turbulent, as in the case of gravitational convection. On the other hand, in contrast to gravitational convection, there may be considerable stability to displacements orthogonal to the slantwise flow and this may inhibit mixing. In the hydrostatic limit, the convective flow will be nearly horizontal, and displacements orthogonal to the flow will be essentially vertical. From (12.2.16), these will feel a stability nearly equal to N^2. Unfortunately, there are very few direct observations or laboratory experiments of slantwise convection.

As in the case of gravitational convection, a CAPE-like quantity may be defined for slantwise convection, giving the total amount of potential energy available for conversion to kinetic energy following the displacement of a tube of air. Consider the work done in displacing a tube of air, labeled i, to some point a in x–z space. The work done, per unit mass, during this displacement is

$$W = \int_i^a \left(\frac{\mathbf{F}}{m}\right) \cdot d\boldsymbol{l} = \int_i^a \frac{d\mathbf{V}}{dt} \cdot d\boldsymbol{l}, \tag{12.2.40}$$

where m is the mass of the sample and $d\boldsymbol{l}$ is a unit distance along the displacement. Using (12.2.8) and (12.2.9) for the accelerations, (12.2.40) becomes

$$W = \int_i^a \left[f(M_t - M_g)\hat{i} + \Gamma(s_t - s_e)\hat{k}\right] \cdot d\boldsymbol{l}, \tag{12.2.41}$$

where $\hat{i}$ and $\hat{k}$ are unit vectors in the x and z directions. To evaluate (12.2.41), we need to know the endpoint a. At first, it might seem that one also needs to know the path of integration in order to evaluate (12.2.41). But a well-known theorem of vector calculus states that *the evaluation of a line integral, such as (12.2.41), is independent of the path of integration if the integrand is irrotational.* This is easy to prove. Suppose we integrate the vector field $\mathbf{A}$ along two different paths l_1 and l_2:

$$W_1 = \int_i^a \mathbf{A} \cdot d\boldsymbol{l}_1,$$

$$W_2 = \int_i^a \mathbf{A} \cdot d\boldsymbol{l}_2.$$

The difference between these evaluations is

$$W_1 - W_2 = \int_i^a \mathbf{A} \cdot d\boldsymbol{l}_1 - \int_i^a \mathbf{A} \cdot d\boldsymbol{l}_2 = \oint \mathbf{A} \cdot d\boldsymbol{l},$$

where the closed line integral goes up path 1 and comes down path 2. But by the Stokes theorem,

$$W_1 - W_2 = \oint \mathbf{A} \cdot d\boldsymbol{l} = \iint (\nabla \times \mathbf{A}) \cdot \hat{n} d\sigma,$$

where $\hat{n}$ is a unit vector normal to the area enclosed by the curve and $d\sigma$ is a differential area under the curve. Thus, if $\nabla \times \mathbf{A} = 0$, $W_1 = W_2$ and the line integral is independent of the path.

In (12.2.41), M_t and s_t are constants. Thus the curl of the integrand is

$$f\frac{\partial M_g}{\partial z} - \Gamma\frac{\partial s_e}{\partial x} = 0,$$

by the thermal wind equation (12.2.13).

Thus the evaluation of W depends only on the endpoint a. We may, if we so desire, evaluate (12.2.41) by integrating along the tube's M surface, where $M_g = M_t$. Then

$$W = \int_i^a \Big|_M \Gamma(s_i - s_e)\, dz, \tag{12.2.42}$$

as long as a lies on the M surface. The notation $\Big|_M$ reminds us that the integral is taken on an M surface.

Now referring to Figure 12.3, it is evident that $s_i > s_e$ along the M surface between points B and D. Thus W is maximized in (12.2.42) if we take point a to be point D in Figure 12.3, the *point of neutral buoyancy (PNB)*. [If we had integrated (12.2.41) along the s surface instead, we would still find that W is maximized by taking point a to be point D.] In analogy with CAPE, we define this maximum potential energy as the *slantwise convective available potential energy,* or SCAPE_i for short:

$$\text{SCAPE}_i = \int_i^{\text{PNB}} \Big|_M \Gamma(s_i - s_e)\, dz. \tag{12.2.43}$$

If we go back to the original definition of buoyancy, and include the corrections for the effect of water substance on density, a more general definition would be

$$\begin{aligned} \text{SCAPE}_i &= \int_i^{\text{PNB}} \Big|_M g\left(\frac{\alpha_i - \alpha_e}{\alpha_e}\right) dz, \\ &= \int_{p_i}^{\text{PNB}} \Big|_M -(\alpha_i - \alpha_e)\, dp, \\ &= \int_{\text{PNB}}^{p_i} \Big|_M R_d(T_{\rho i} - T_{\rho e})\, d\ln p, \end{aligned} \tag{12.2.44}$$

where $T_{\rho i}$ and $T_{\rho e}$ are the density temperatures of the tube and its environment, respectively. Comparison to Eq. (6.3.5) shows that this is the same as the definition of CAPE_i, except the evaluation is made on M surfaces rather than along the vertical. When the atmosphere is barotropic, M surfaces are vertical and so in this special case, $\text{SCAPE}_i = \text{CAPE}_i$. Thus, the SCAPE of the tube is the more complete definition of its potential energy, as it includes the centrifugal as well as gravitational potential of the tube.[2]

Another way of evaluating SCAPE_i is to choose the integration path to consist of two legs: a purely vertical leg extending from the sample's position vertically to the pressure of its PNB, and a purely horizontal leg extending from this point to the PNB itself. Thus

$$\begin{aligned}\text{SCAPE}_i &= \int_{\text{PNB}}^{p_i} R_d(T_{\rho i} - T_{\rho e})\, d\ln p + \int_{x_i}^{x_i - L} f(M_i - M_g)\, dx, \\ &= \text{CAPE}_i^{\text{PNB}} + \int_{x_i}^{x_i - L} f(M_i - M_g)\, dx, \end{aligned} \tag{12.2.45}$$

where $\text{CAPE}_i^{\text{PNB}}$ is the CAPE_i of the sample lifted to pressure PNB (which is *not,* in general, its LNB) and L is the horizontal distance from the x position of the original sample, x_i, to the PNB. Since $M_{\text{PNB}} = M_i$,

$$v_{\text{PNB}} + f x_{\text{PNB}} = v_i + f x_i,$$

or

$$L = x_i - x_{\text{PNB}} = \frac{v_{\text{PNB}} - v_i}{f}. \tag{12.2.46}$$

The second integral in (12.2.45) can be approximately evaluated using integration by parts:

$$\begin{aligned}\int_{x_i}^{x_i - L} f(M_i - M_g)\, dx &= \int_{x_i}^{x_i - L} f\, d\left[(M_i - M_g)x\right] + \int_{x_i}^{x_i - L} f x\, dM_g \\ &= fL(M_n - M_i) + \int_{x_i}^{x_i - L} f x \frac{\partial M_g}{\partial x} dx \\ &= fL(M_n - M_i) - \frac{1}{2} f L^2 \overline{\eta}_g, \end{aligned} \tag{12.2.47}$$

where M_n is the absolute momentum evaluated at the pressure of PNB but at the initial horizontal position of the sample, x_i,

$$M_n \equiv M_g(x_i, \text{PNB}),$$

---

[2] Note that M is proportional to the *geostrophic coordinate* X, used in semi-geostrophic theory, so that SCAPE is the CAPE of samples lifted vertically in geostrophic space.

and $\overline{\eta}_g$ is the average absolute geostrophic vorticity at the pressure of the PNB between x_i and $x_i - L$. If we make the approximation

$$L\overline{\eta}_g \simeq Lf + v_n - v_{\mathrm{PNB}},$$

then, using (12.2.46) for L, (12.2.47) becomes

$$\int_{x_i}^{x_i - L} f(M_i - M_g) \simeq \frac{1}{2}(v_{\mathrm{PNB}} - v_i)(v_n - v_i).$$

Thus (12.2.45) may be written

$$\mathrm{SCAPE}_i \simeq \mathrm{CAPE}_i^{\mathrm{PNB}} + \frac{1}{2}(v_{\mathrm{PNB}} - v_i)(v_n - v_i). \tag{12.2.48}$$

In a baroclinic atmosphere, $v_{\mathrm{PNB}}^2 > v_i^2$ and $v_n^2 > v_i^2$, so that *$SCAPE_i$ is always greater than or equal to $CAPE_i^{\mathrm{PNB}}$*. If the atmosphere is stable to gravitational convection, $\mathrm{CAPE}_i^{\mathrm{PNB}}$ will be negative, but SCAPE_i may still be positive. If $\mathrm{CAPE}_i^{\mathrm{PNB}}$ is positive, indicating an atmosphere that is unstable to gravitational convection, then SCAPE_i will also be positive, and in general, greater than CAPE_i (which, even in this case, will not usually be equal to $\mathrm{CAPE}_i^{\mathrm{PNB}}$). The second term on the right side of (12.2.48) is the mean flow kinetic energy available for conversion into slantwise convective motion. In strongly baroclinic atmospheres, this may contribute on the order of 1000 J kg^{-1} of energy to SCAPE_i.

12.3 Observational evidence of slantwise convection

The parcel theory of slantwise convection shows that the motions should assume the form of sloping circulations along neutral-buoyancy surfaces. In the case of conditional instability to moist slantwise convection, application of the slice method (Section 6.5) shows that the motion should consist of thin, ascending sheets of cloudy air interspersed with thicker layers of unsaturated, more slowly descending air, though partial evaporation of precipitation falling from the ascending sheets should drive stronger, sloping downdrafts. The horizontal scale of the convection in all cases scales as

$$L \sim \frac{\Delta v}{f}, \tag{12.3.1}$$

where Δv is the shear of the ambient wind across the depth of the unstable layer. For typical atmospheric values of Δv and f, this is of order 100 km, so that slantwise convection is considered to be a *mesoscale* phenomenon. Note also that the *Rossby number* based on L is of order unity; this may be regarded as a dynamic definition of mesoscale.

When and where would we expect slantwise convection to occur? As in gravitational convection, we may distinguish between triggered and statistical equilibrium convection. In the former case, large amounts of SCAPE_i

should be in evidence before the convection occurs, and the convection could be triggered by any of a number of conditions, such as low-level ascent and removal of a temperature inversion. In the latter case, we would expect the convection to occur when and where other physical processes tend to destabilize the atmosphere to slantwise convection, and in analogy with gravitational convection, we should expect this to occur in conditions very close to neutrality (zero SCAPE_i).

Also in analogy to gravitational convection, we can define a state of *potential instability* (see Section 6.7) as one in which θ_e decreases upward along M surfaces. This does *not* imply positive values of SCAPE, nor does it imply the existence of available potential energy (Section 6.6) for slantwise convection. But if a potentially unstable air mass is bodily lifted to saturation, the potential instability can be converted to actual instability. In statistical equilibrium, the activity of convection will be related to the rate at which potential instability is converted to SCAPE.

Often, the warm sectors of baroclinic cyclones are potentially unstable to either or both slantwise and gravitational convection. As this air rises over frontal systems, the instability is converted to slantwise, and perhaps gravitational, parcel instability. (If the atmosphere is baroclinic, slantwise instability will always appear before gravitational instability, but if the forcing is strong, slantwise convection may not be able to prevent the atmosphere from progressing into a gravitationally unstable state.) Thus the ascent regions of baroclinic cyclones may often exhibit slantwise convection.

One manifestation of slantwise convection might be the multiple layers of sloping sheets of cloud observed ahead of warm fronts. Although these are very much what one might expect to see, there are no quantitative studies that prove or disprove this conjecture, at the time of this writing.

Precipitation in baroclinic cyclones is often organized into mesoscale bands, which may not always be direct manifestations of frontal circulations. An example of such bands is presented in Figure 12.5. A review of the mechanisms proposed to explain such features is provided by Parsons and Hobbs (1983). Although there is much circumstantial evidence that some of these mesoscale bands are manifestations of slantwise convection, there has been no direct evidence proving it.

The strongest circumstantial evidence for the occurrence of slantwise moist convection in the atmosphere is the observation that large regions of baroclinic flow are almost exactly neutral to slantwise ascent (Emanuel, 1988); presumably, this is not a coincidence but an indication that slantwise convective adjustment has occurred or is occurring. Figure 12.6 shows an example of a baroclinic flow in which a condition of slantwise convective neutrality was observed by flying an instrumented aircraft downward along an M surface, indicated by the bar in the figure. The sounding is shown together with a vertical sounding in Figure 12.7. The M-surface sounding falls along a moist adiabat, indicating neutrality to slantwise convection, while a vertical sounding through the midpoint of the M-surface sounding

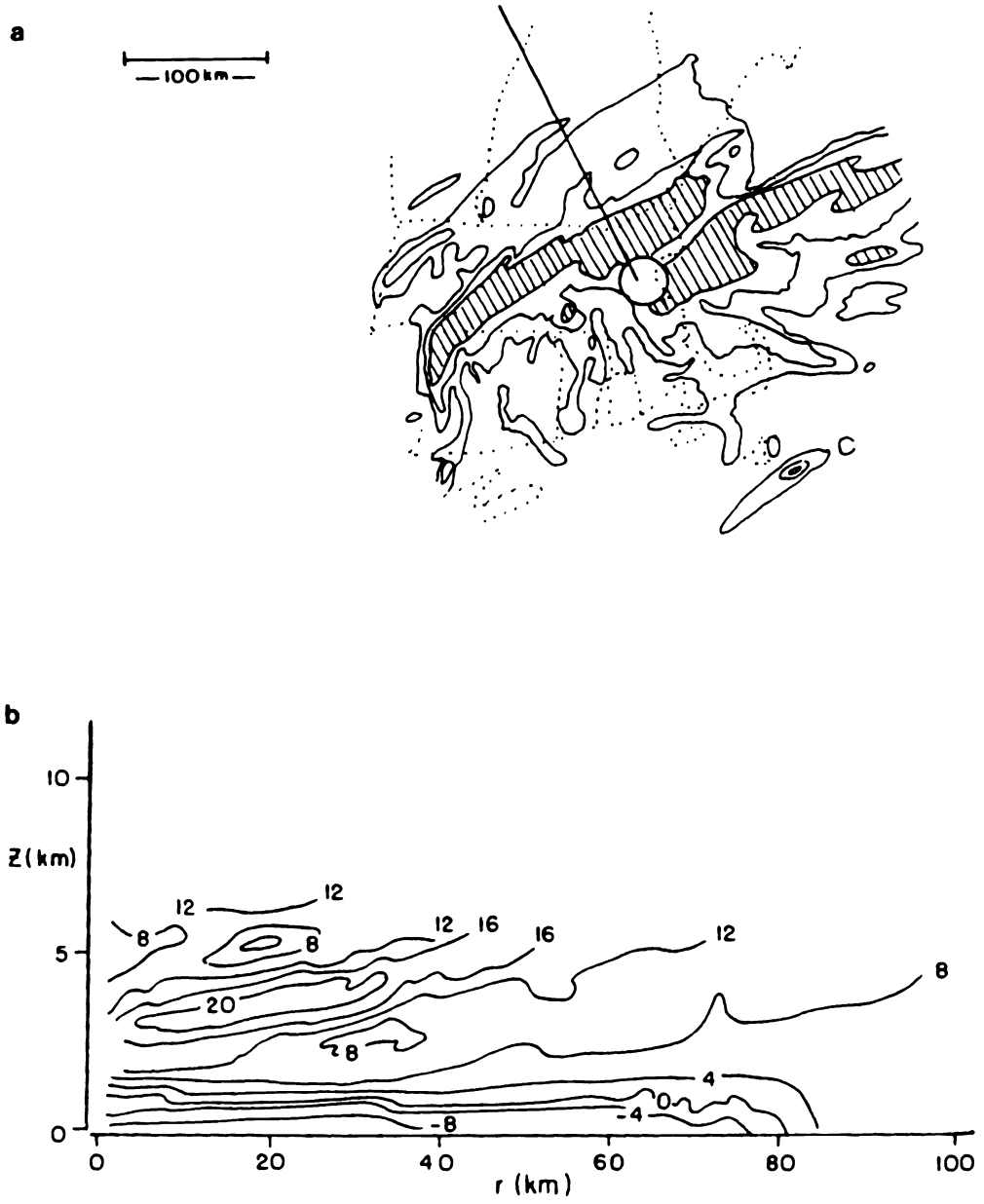

Fig. 12.5 Constant altitude display (a) of radar reflectivity (dBZ) in a layer from 2 to 4 km from a radar located in Cambridge, Massachusetts, at 0729 GMT February 12, 1983. Hatched regions show reflectivity greater than 30 dBZ. Heavy line shows location of vertical cross section in (b), which shows the Doppler-derived radial component of velocity (m s^{-1}), with positive values indicating flow away from the radar.

is clearly quite stable.

Figure 12.8 shows a vertical cross section through the same flow, showing the distribution of M and θ_e^* surfaces, as well as surfaces of constant θ_e. The stippled region is characterized by parallel M and θ_e^* surfaces, indicating moist adiabatic lapse rates on M surfaces and slantwise neutrality. But the θ_e cross section shows regions of negative θ_e gradient along M surfaces, indicating potential (but not parcel) instability. Evidently, the slantwise convection was efficient enough in this case to eradicate instability as fast as the large-scale frontal ascent acted to generate it through the conver-

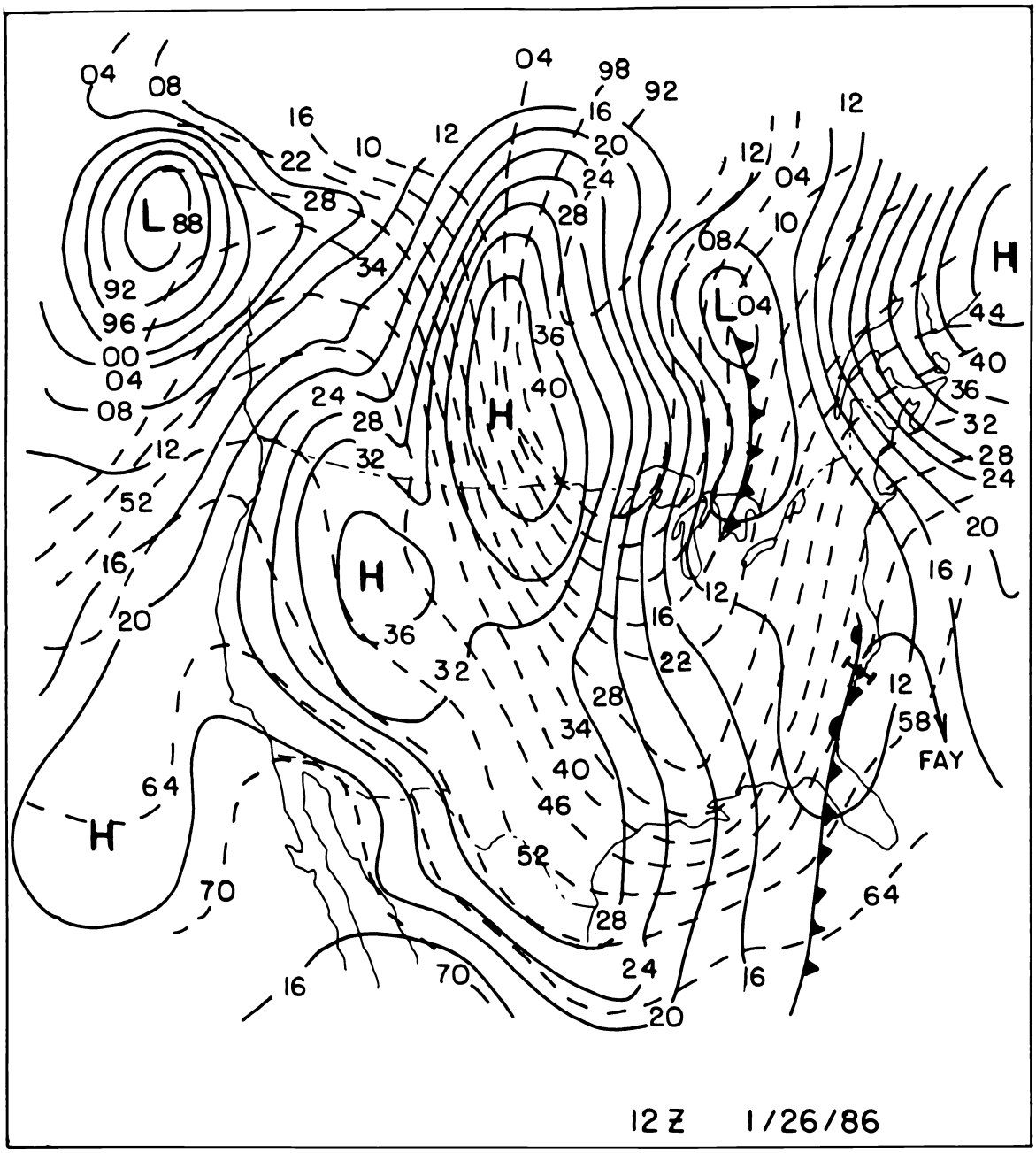

Fig. 12.6 Surface pressure (solid lines) and 1000 to 500-millibar thickness (dashed lines) at 1200 GMT January 26, 1986. Heavy bar through Fayetteville, North Carolina (FAY), shows path of *M*-surface sounding in Figure 12.7.

sion of potential instability. Thus the convection in this case was almost certainly of the statistical equilibrium kind. The observations suggest that slantwise convection almost always occurs in conjunction with large-scale cyclonic systems and may be difficult to separate from motions directly produced by frontogenesis.

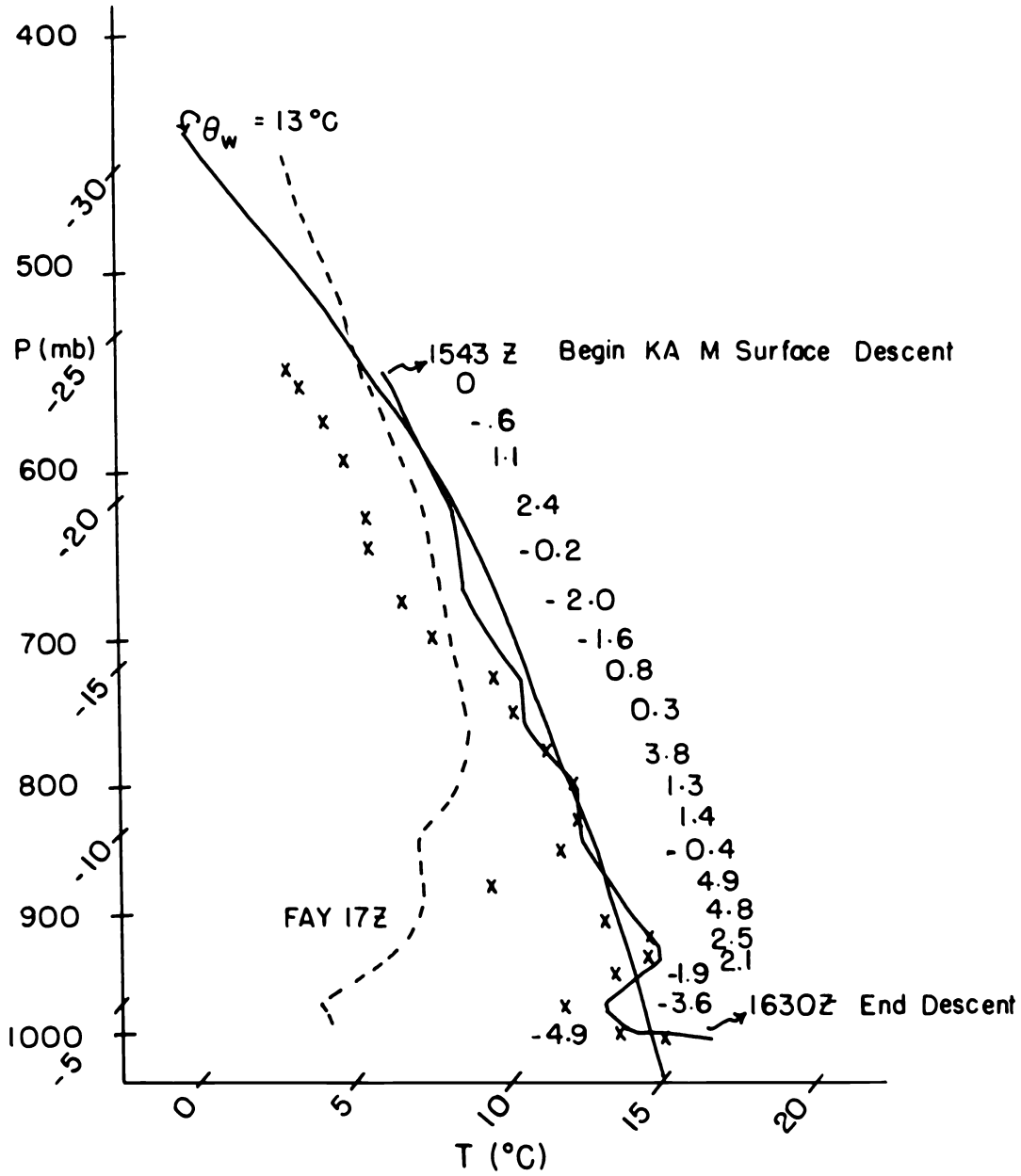

Fig. 12.7 M-surface sounding by instrumented aircraft between 1543 and 1630 GMT January 26, 1986. Solid line shows temperature and ×'s denote dew-point temperature. Heavy solid line is a pseudoadiabat. Numbers to right of sounding indicate departures of M (m s^{-1}) from initial value. Dashed line shows vertical temperature sounding at Fayetteville, North Carolina, at 1700 GMT.

EXERCISES

12.1 An incompressible fluid is rotating with a constant angular velocity Ω. What is the oscillation frequency of a small ring of fluid displaced radially in this flow?

12.2 Linearize the strictly incompressible, inviscid momentum equations about a resting state on an f plane. Find an expression for the oscillation frequency of small disturbances that vary sinusoidally in all three spatial directions. What combination of wavenumbers makes the oscillation frequency the same as that derived from parcel theory? Can

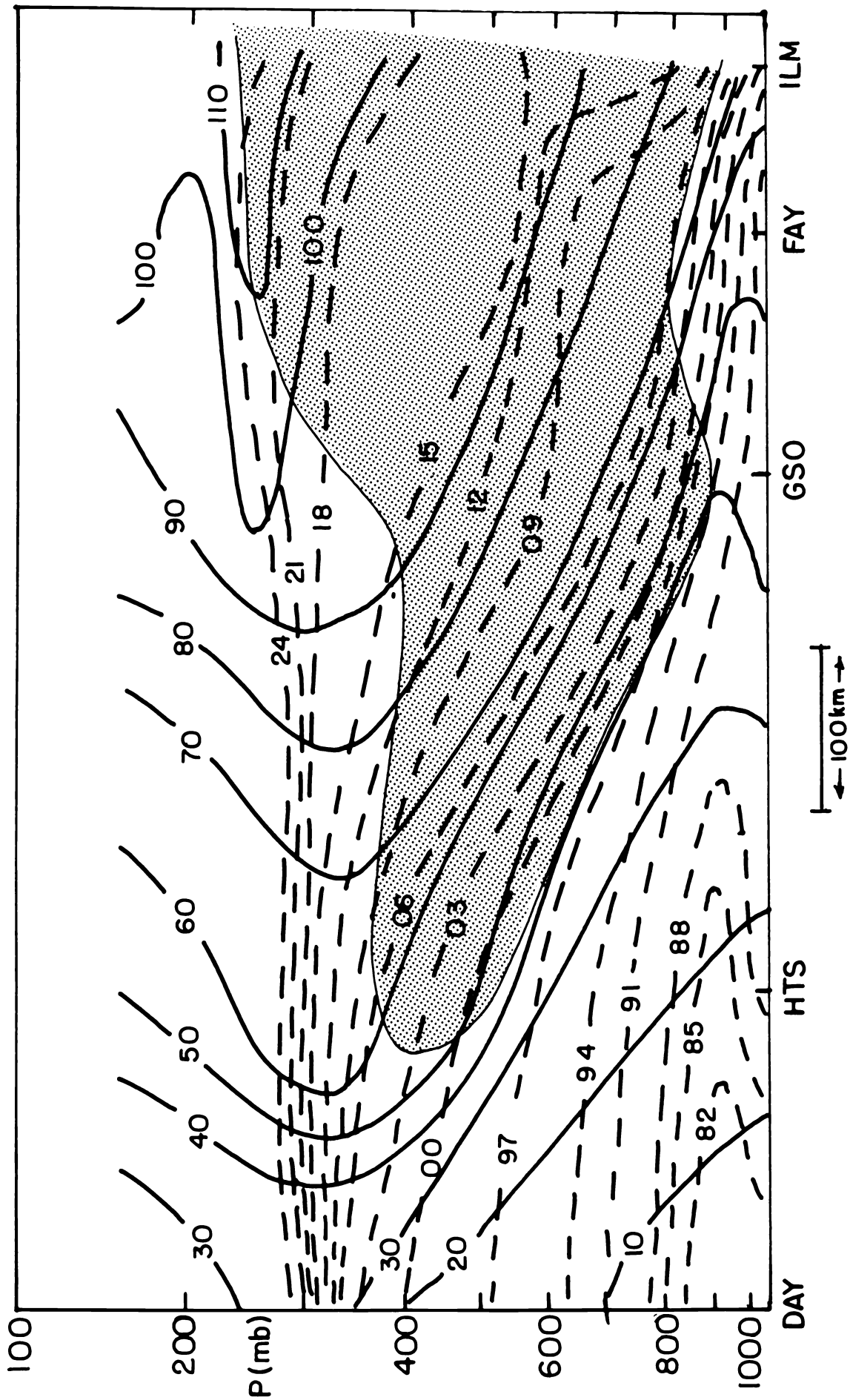

Fig. 12.8 Cross sections from Dayton, Ohio (DAY), through Huntington, West Virginia (HTS), and Greensboro (GSO), Fayetteville (FAY), and Wilmington (ILM), North Carolina, constructed from vertical soundings at the indicated cities. Solid lines in both panels

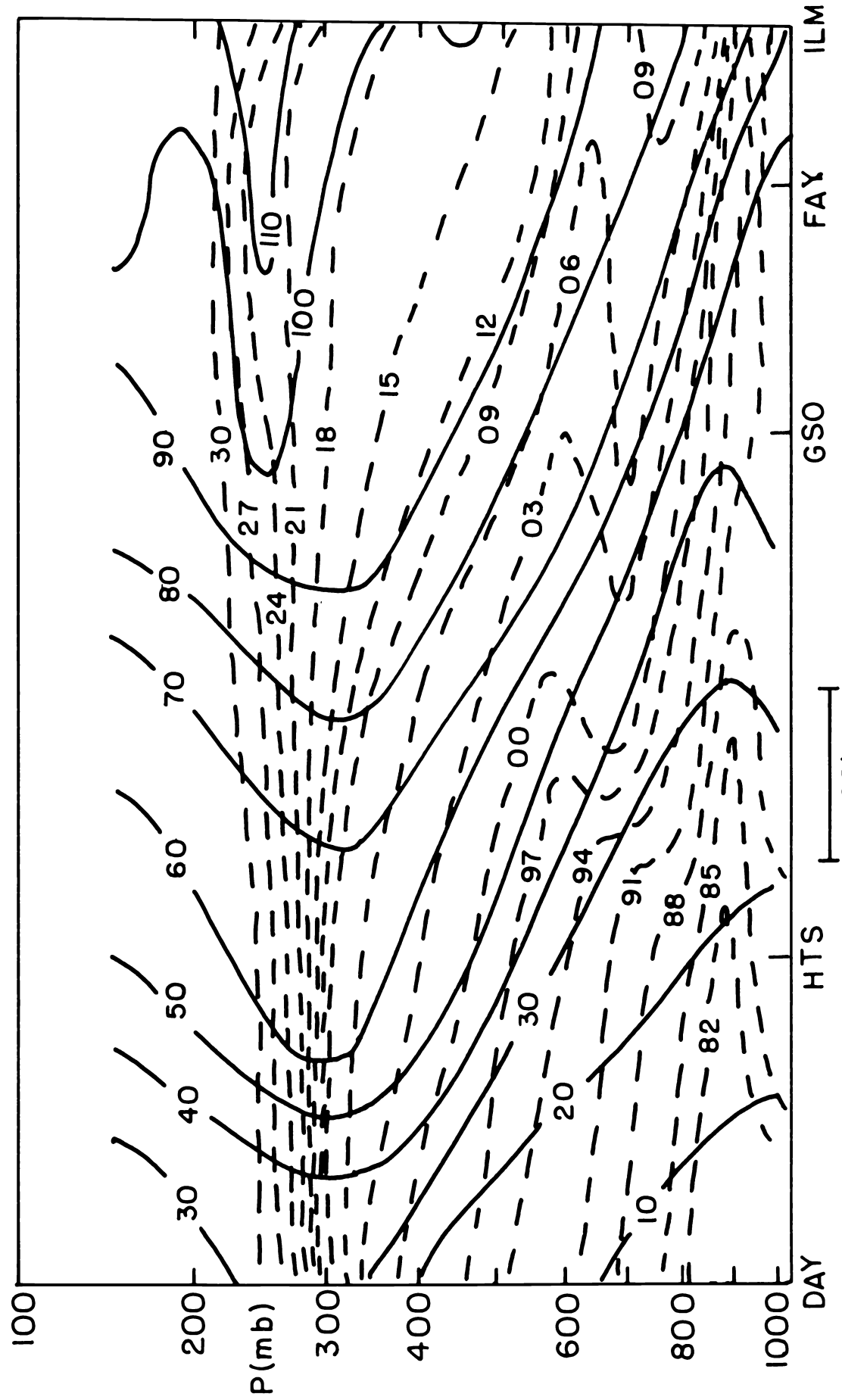

show M (m s^{-1}); dashed lines in (a) depict θ_e^* (K) and in (b) depict θ_e (K). Stippling in (a) denotes regions of approximately moist adiabatic lapse rates on M surfaces.

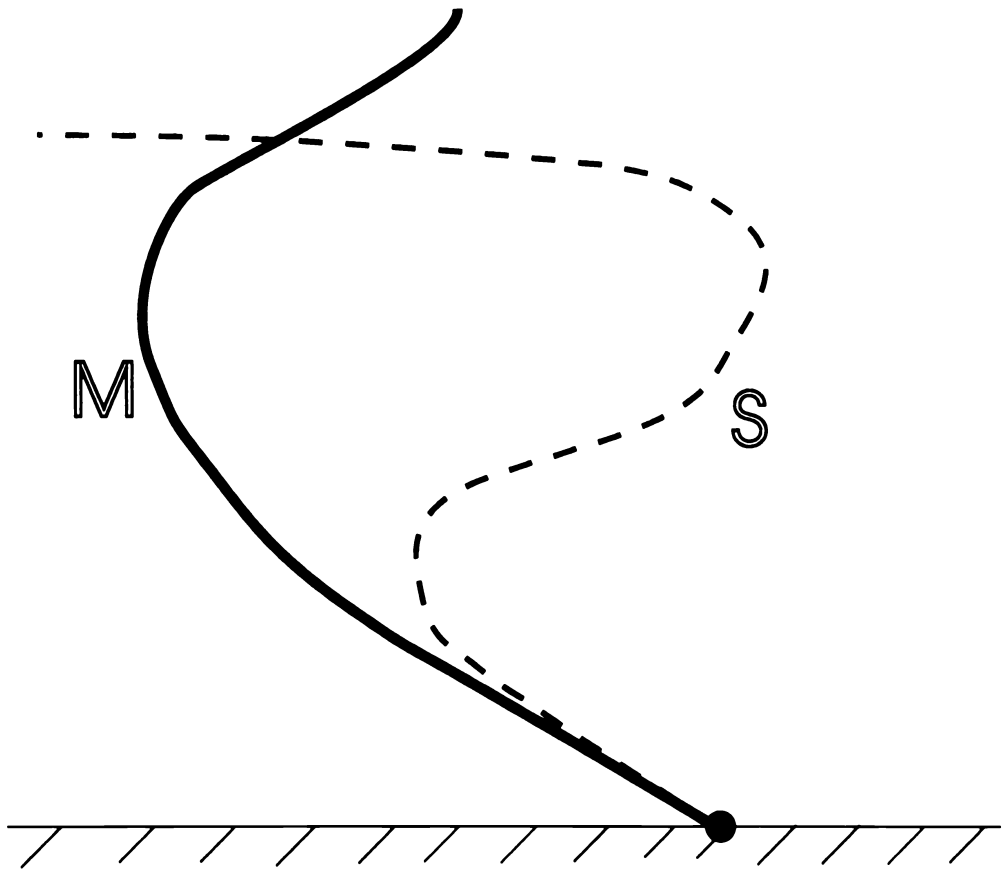

Fig. E12.1 Hypothetical configuration of M surface (solid line) and neutral-buoyancy surface (dashed line) for a sample located at bottom right.

you explain this in terms of perturbation pressure gradients?

12.3 Consider the displacement of a small tube of air aligned along the direction of the thermal wind, which may be considered constant, following the analysis of Section 12.2. Find expressions for the motion of the tube in the case that $N^2 = 0$. What direction of the tube's motion eliminates oscillations? Supposing that there is a lid at $z = H$, find the magnitude of the motion when the tube reaches the location where its value of M equals that of its environment.

12.4 Show that the requirement for slantwise instability in a dry atmosphere, given locally by (12.2.30), is equivalent to $fq < 0$, where q is the *potential vorticity,* defined

$$q \equiv \alpha(f\hat{k} + \nabla \times \mathbf{V}) \cdot \nabla\theta.$$

Potential vorticity is conserved in adiabatic, inviscid flows. How does an atmosphere that is unstable to dry slantwise convection become stable?

12.5 Figure E12.1 shows the configuration of an M surface and a surface along which the particular sample shown would be neutrally buoyant if displaced adiabatically (including the effects of condensation of water). Describe qualitatively the trajectory of the indicated sample and the nature of the ensuing convection.

REFERENCES

Emanuel, K. A., 1983a: The Lagrangian parcel dynamics of moist symmetric instability. *J. Atmos. Sci.*, **40,** 2368–2376.

_____, 1983b: On assessing local conditional symmetric instability from atmospheric soundings. *Mon. Wea. Rev.*, **111,** 2016–2033.

_____, 1988: Observational evidence of slantwise convective adjustment. *Mon. Wea. Rev.*, **116,** 1805–1816.

Parsons, D. B., and P. V. Hobbs, 1983: The mesoscale and microscale structure and organization of clouds and precipitation in mid-latitude cyclones. VII: Formation, development, interaction and dissipation of rainbands. *J. Atmos. Sci.*, **44,** 559–579.